Chapter 3
Case Study of Self-Healing in Metallic Composite with Embedded Low Melting Temperature Solders

In the preceding chapter, we discussed the general principles of the thermodynamics of self-healing with the emphasis on metallic materials. In this chapter, we concentrate on the multiscale nature of self-healing mechanisms. To illustrate the multiscale nature of entropy production, we investigate a particular example of grain growth in metals. After that we discuss a prototype system involving an Al alloy reinforced with microtubes, filled with Sn60Pb40 solder; this is discussed as a case study.

3.1 Introduction

Wear occurs at most solid surfaces that come in contact with other solid surfaces. While biological surfaces and tissues usually have the ability to repair minor wear damage, engineered self-healing materials only started to emerge recently. An example of a smart self-healing material is the material with imbedded microcapsules or microtubes, which rupture during crack propagation and release a healing agent that repairs the crack. Self-healing mechanisms are hierarchical in the sense that they involve interactions with different characteristic scale lengths. While traditional models of self-healing require equations with many degrees of freedom, taking into account the hierarchical organization allows us to reduce the number of equations to a few degrees of freedom. We discuss the conditions under which the self-healing occurs and provide a general theoretical framework and criteria for self-healing using the concept of multiscale organization of entropy and nonequilibrium thermodynamics (Table 3.1).

Self-healing is defined as the ability of a material or surface to heal (recover or repair) damages automatically or autonomously (Ghosh 2009). Self-healing has become an object of active investigation in recent years (Balazs 2007; Zwaag 2007; Wool 2008; Ghosh 2009; Nosonovsky and Bhushan 2008a, 2009), whereas polymers have been the main focus of these studies (Chen et al. 2002; Hayes et al. 2007; Cordier et al. 2008). Self-healing materials including metals (Lumley 2007;

M. Nosonovsky and P.K. Rohatgi, *Biomimetics in Materials Science: Self-Healing, Self-Lubricating, and Self-Cleaning Materials*, Springer Series in Materials Science 152, DOI 10.1007/978-1-4614-0926-7_3,

Table 3.1 Multiscale framework for properties of metals (Nosonovsky and Esche 2008b)

Scale	Characteristic size	Entropy	Simulation method	Input	Output
Macro	Specimen	Increases	Finite Element Method	Yield strength	Deflections, stresses
Micro (meso)	Grain	Decreases	Monte Carlo Method	Parameters of (3.4)	Grain size
Molecular	Crystal lattice	Increases	Molecular Dynamics	Position of atoms	Position of atoms, parameters of (3.4)

Manuel 2009), ceramics (Nakao et al. 2009), and their composites as well as coatings (Sloof 2007; Zheludkevich 2009) are also investigated.

Several design strategies have been suggested so far for self-healing metals. These strategies include the release of a healing agent (e.g., capsules that are ruptured during crack propagation and release a liquid that "glues" the crack opening), circulation of a liquid healing agent (similar to the vascular blood circulation in humans and animals), a mixture of a low melting point solder with a high melting point alloy, reinforcement of the material with shape-memory alloys (SMA), nanoparticle migration, etc. In some cases, an external intervention such as heating is required to initiate healing (e.g., to cause melting of the healing agent or the restoration of the original shape of the SMA), while other self-healing systems are intended to act autonomously (Ghosh 2009).

There are several computational and analytical models for particular mechanisms of self-healing (Balazs 2007; Wang et al. 2007b; Lucci et al. 2008a, b, c; Manuel 2009; Remmers and de Borst 2007; Vermolen et al. 2007). Most of these models apply mechanical and hydrodynamic equations for crack propagation and propagation of the healing agent. They can be used to build a computational model such as a finite element (FE), computational fluid dynamics (CFD), or molecular dynamic (MD) analysis. However, most of these models are ad hoc and dependent on a particular shape of voids and cracks. In this chapter, the development of a general model using the physical principles of self-healing is presented.

Self-healing is, in a sense, opposite to degradation processes such as wear, fatigue, and creep. Many of these processes occur at the surface or in the subsurface layer, involving dry friction and wear and other dissipative processes that occur during sliding of two solid surfaces (Bryant et al. 2008; Nosonovsky and Bhushan 2009). The main characteristic of a dissipative process is irreversibility; or, from the thermodynamic point of view, the production of entropy. Self-healing may be viewed in the broader context of self-organization. Recent studies have shown that nonequilibrium thermodynamic processes during friction can lead to self-organization and the formation of secondary structures that result in a significant reduction of friction and wear (Fox-Rabinovich and Totten 2006; Fox-Rabinovich et al. 2007; Nosonovsky and Bhushan 2009; Nosonovsky 2010b). In this chapter,

we suggest a thermodynamic analysis of self-organization and self-healing during friction and consider a case study of void self-healing in plant leaves that serves as an inspiration for biomimetic self-healing coatings.

3.2 Modeling Self-Healing

3.2.1 Multiscale Effects of Crystal Grain Growth

It is generally accepted that physical, chemical, and mechanical properties of crystalline materials can, in principle, be deduced from their microstructure. However, in practice, it is very difficult to predict such properties as the modulus of elasticity, Poisson's ratio, yield strength, and hardness because they are a result of various, often random, factors, and interactions at different length scales, from the macroscale down to the mesoscale and molecular scale. Similarly to other dissipative systems of physical chemistry that involve interaction at various length scales, such as the wetting of rough solids (Nosonovsky and Bhushan 2007b), a multiscale method for simulating grain growth is needed. Modeling a material's mechanical behavior at the macroscale usually involves continuum solid state mechanics (elasticity and plasticity) and corresponding computational methods such as the finite element method (FEM), and the boundary element method (BEM). At the mesoscale level, the imperfections of the lattice structure, such as grains, dislocations and defects, define a characteristic length scale, and stochastic simulation methods, such as the Monte Carlo (MC) method, are used. At the molecular level, molecular dynamics (MD) simulation can be applied. Therefore, a multiscale framework is needed to analyze the mechanical properties.

In order to provide a cross-scale linkage, a material property model has to be used (Fig. 3.1a). The property model relates the mesoscale level of description with the macroscale material properties. In particular, the average grain size r is the parameter that affects the yield strength σ_{Y} of the material. There are several models that relate the grain size with the yield strength. The classical Hall–Petch model of grain boundary strengthening developed in 1950s states that the yield strength decreases with growing grains as

$$\sigma_{\mathrm{Y}} = \sigma_{\mathrm{Y0}} + \frac{k}{\sqrt{r}}, \tag{3.1}$$

where σ_{Y0} is the limiting value corresponding to large grains and k is a constant coefficient (Hall 1951). The reasoning behind the Hall–Petch relationship is similar to that of the linear elastic fracture theory, which states that the stress intensity factor is proportional to the square root of the crack size. In order to initiate yielding, the value of $(\sigma_{\mathrm{Y}} - \sigma_{\mathrm{Y0}})\sqrt{r}$ should reach a certain critical threshold similarly to the crack growth initiation.

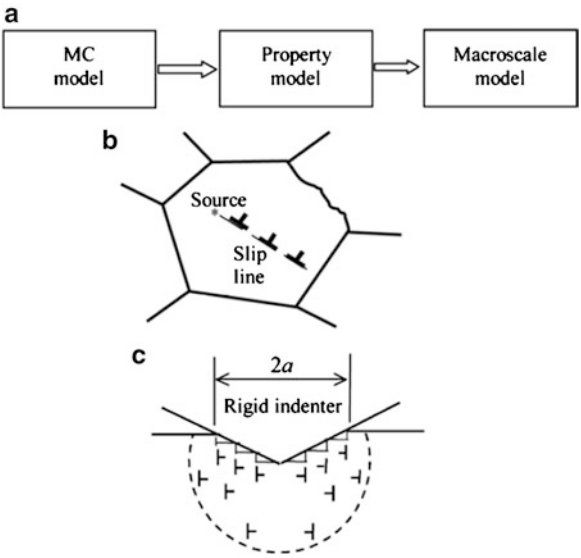

Fig. 3.1 (**a**) Multiscale modeling for material processing and properties, (**b**) scale effect in Hall–Petch theory, (**c**) strain gradient plasticity theory (Nosonovsky and Esche 2008b)

According to the Taylor model of plasticity, dislocations are emitted from Frank–Read sources and move along a slip plane that is common to many dislocations (Fig. 3.1b). Due to their interaction with each other, the dislocations may become stuck in the Taylor network, but when the externally applied stress exceeds the Peierls stress of the dislocations σ_{p}, they start to move and plastic yielding is initiated. The number of dislocations at a particular pile in a grain is proportional to the average grain size r and to the applied stress, while the total stress at the lead dislocation σ_{L} is proportional to the number of dislocations and the applied stress. Therefore, it can be easily shown that to initiate yielding $(\sigma_L > \sigma_{\mathrm{p}})$, the value of the applied stress should be proportional to $\sqrt{r}$ (Friedman and Chrzan 1998).

The Hall–Petch relationship predicts that the yield strength can increase with decreasing grain size without limit. However, very small grains with sizes comparable with that of the dislocations do not provide high strengths. In the past decade, the inverse Hall–Petch relationship has been suggested theoretically and studied experimentally for nanocrystalline materials with submicron grain sizes, and there is experimental evidence of grain boundary softening, below grain size of 10 nm.

Several models of strain gradient plasticity that emerged since the 1990s predict that the yield strength σ_{Y} is scale dependent and decreases with the decreasing characteristic size l of the system as:

$$\sigma_{\mathrm{Y}} = \sigma_{\mathrm{Y0}} \sqrt{1 + \frac{l_0}{l}}, \tag{3.2}$$

where l_0 is a material parameter that characterizes the average distance that dislocations can glide. The phenomenological explanation of the scale dependence of the yield strength is that smaller volumes of a material have fewer defects and

dislocations, which makes the material stronger. This idea is illustrated in Fig. 3.1c, which shows that dislocations are needed to accommodate for strain compatibility during the indentation deformation. Both the number of needed dislocations and the average length of dislocation loops are proportional to the contact radius l, with the volume being proportional to l^3. The density of dislocations (total length of all loops per unit volume) is thus proportional to $1/l$. According to the Taylor relation, the yield strength is proportional to the square root of the dislocation density. Thus, $\sigma_Y \sim l^{-1/2}$, which is equivalent to (3.2) for $l << l_0$ (Nix and Gao 1998; Hutchinson 2000). In other words, for an indenter of small size, the volume where the dislocations are created is not large enough to accommodate the surface deformation. This gives rise to the size-dependent strengthening predicted by the strain-gradient plasticity.

Normally, l_0 is a material parameter associated with the average distance that dislocations can glide, and it is of the order of 1 μm (Hutchinson 2000). However, for small grains, the grain size defines the distance that the dislocations can glide. Therefore, it may be assumed that $r = l_0$, and the strain gradient plasticity approach predicts grain boundary softening similarly to the inverse Hall–Petch relationship. The length scale at which the transition from the Hall–Petch to inverse Hall–Petch relationship occurs is estimated to be between dozens and hundreds of nanometers (Friedman and Chrzan 1998; Conrad and Narayan 2000).

The grain size in metals is determined by thermally activated grain growth processes and by recrystallization caused by applied stresses. Due to the misorientation of atoms in neighboring grains, there is excess energy associated with the grain boundaries, and therefore the grain growth is driven by the reduction of the energy. The grain growth is a thermally activated random process similar to diffusion, and thus the kinetics of the grain growth is dependent on the temperature (Nosonovsky and Esche 2008b).

The Monte Carlo (MC) method is widely used to simulate the grain growth. In this method, a 2D or 3D lattice is initiated by assigning a random orientation to every lattice site. An energy functional is selected to account for the misorientation of neighboring sites. Subsequently, at every MC step, an attempt is made to randomly change the orientation, and the energy of the new configuration is compared with the energy of the initial configuration. If the energy decreases as a result of the reorientation, the new orientation is accepted. A grain is defined as a group of neighboring sites with the same orientation. Since the periodicity of the MC simulation lattice is much greater than the atomic size, a scaling procedure is needed to relate the MC lattice spacing to physical size units and the MC steps to physical time units (Nosonovsky and Esche 2008b).

The MC simulation method can be applied for various phenomena such as normal grain growth in 2D or 3D and recrystallization, with varying temperature, anisotropic material, etc. The normal isotropic grain growth at constant temperature represents a convenient example because it has a theoretical solution for the average grain size, with the parabolic dependence of the average grain radius r on time t:

$$r = C\sqrt{t}, \tag{3.3}$$

Table 3.2 Hierarchy levels in the physical system and simulation (Nosonovsky and Esche 2008b)

	Physical system			Simulation		
	Objects	Driving force	Entropy	Objects	Driving force	Entropy
Macroscale	Continuum	material	–		$\Delta S_{\text{macro}} = 0$	–
–	–					
Mesoscale	Grains	Decreasing boundary energy	$\Delta S_{\text{meso}} < 0$	Cells	Decreasing energy functional	$\Delta S < 0$
Nanoscale	Atoms	Thermal fluctuations	$\Delta S_{\text{nano}} > 0$	–	–	–

where C is a proportionality constant. The constant can be determined theoretically. Then, (3.3) is given by:

$$r^2 - {r_0}^2 = \frac{4\gamma A Z {V_\text{m}}^2}{{N_\text{a}}^2 h} \exp\left(\frac{\Delta S_\text{f}}{R}\right) \exp\left(-\frac{Q}{RT}\right) t, \tag{3.4}$$

where r_0 is the initial grain size, h is Planck's constant, R is the gas constant, V_m/N_a is the atomic volume, ΔS_f is the activation entropy, Q is the activation enthalpy, γ is the grain boundary energy, A is the accommodation probability, and Z is the average number of atoms per unit area at the grain boundary. However, the uncertainty in the values of the parameters of the (3.4) (especially ΔS_f and Q, which are arguments of the exponential function) is so large that it is more practical to use (3.3) rather than (3.4). The parameters of (3.4) should be obtained from a molecular scale investigation of crystals and then supplied to the mesoscale model for the grain growth (Nosonovsky and Esche 2008b).

It is noted that the MC simulation usually takes into account only the mesoscale level of the physical system (Table 3.2). An interesting consequence of this is that the orderliness of the MC simulation lattice tends to grow, thus leading to a decreasing entropy, which represents an apparent paradoxical contradiction to the second law of thermodynamics, as it discussed in the following section. In the physical system, however, the entropy grows at the molecular level, since the grain boundary migration involves dissipation, thus providing for the overall entropy increase.

MC simulations were shown to provide very close results to those predicted by (3.4) in the case of constant temperature. However, the MC method can also be applied to more complicated phenomena, such as recrystallization, thermo-mechanical processing, and anisotropic grain growth. As the MC simulation results are confirmed by theoretical considerations in the simple case of normal grain growth, it is reasonable to extrapolate the approach for the more complicated cases (Nosonovsky and Esche 2008b).

The temperature T enters into the simulation because the atomic jump frequency that defines the time scale is dependent on T. Therefore, the normalized dependence of the average grain size r on time t has the form

$$r^2 - {r_0}^2 = Kt, \tag{3.5}$$

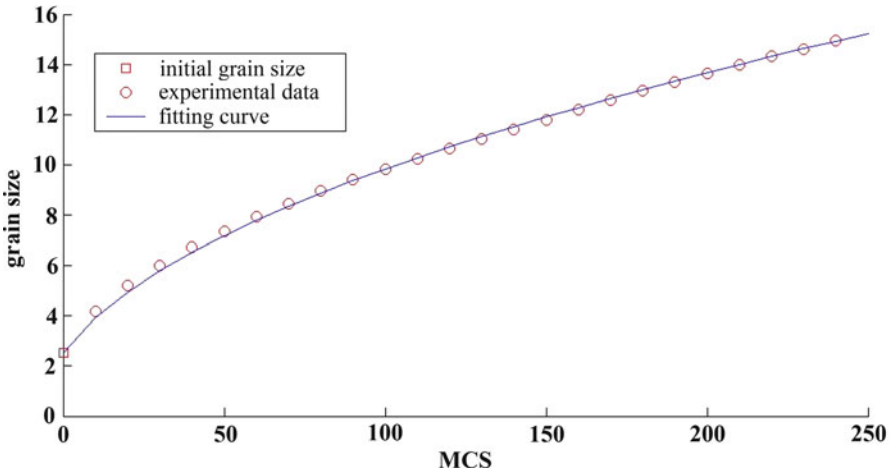

Fig. 3.2 MC simulation results for grain size as a function of time (Nosonovsky and Esche 2008b)

$$K = K_0 \exp\left(-\frac{Q}{RT}\right), \tag{3.6}$$

where K and K_0 are constants.

The MC simulations were started with an initial grain size of $r = 2.5$ and terminated after 242 MC steps when $r \approx 15$ was achieved, so that a significant number of grains were preserved in the lattice. The initial grain size was selected so as to reduce the time needed for grain growth at the initial steps compared with the case of a completely random initial configuration. Ten simulations with different seeds for random number generation were performed and their results were averaged. The microstructure was examined every 10 MC steps. Typical results for the dependence of the average grain size on the simulation time are shown in Fig. 3.2.

The multiscale approach to property simulation involves MC modeling of the grain growth under given conditions and transferring the output to a property model that allows the determination of the yield strength, which in turn is then passed on to a continuum model. In our simulation, we utilized a previously described MC simulation package and the property model based on (3.1)–(3.3). The data can then be transferred to a FEM simulation package or used for the calculation of the deformation of a structural element.

As a simple example, we consider here the twisting of an elastic–plastic rod of radius R under a constant torque τ (Fig. 3.3a). The transition from the elastic to the plastic regime is controlled by the yield strength σ_Y. Assuming that the interior of the rod up to the radius $r = R_0$ is in the elastic state while the exterior $R_0 < r \leq R$ is in the plastic state, the rod can support a torque τ of

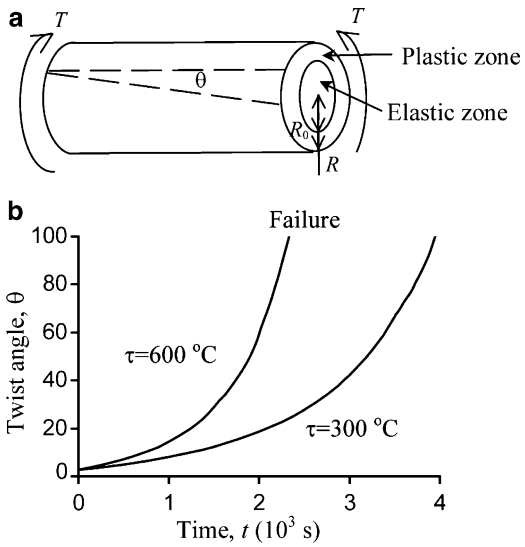

Fig. 3.3 (**a**) An elastic–plastic shaft under torsion, (**b**) twist angle dependence on time (Nosonovsky and Esche 2008b)

$$\tau = L\sigma_{\mathrm{Y}}\frac{{R_0}^2}{3} + L\sigma_{\mathrm{Y}}\frac{R^2 - {R_0}^2}{2} = L\sigma_Y\left(\frac{R^2}{2} - \frac{{R_0}^2}{6}\right). \tag{3.7}$$

From (3.7), $R_0(\tau, \sigma_{\mathrm{Y}})$ is found as

$${R_0}^2 = 3R^2 - \frac{6T}{L\sigma_{\mathrm{Y}}}, \tag{3.8}$$

the polar moment of inertia $J = 0.5\pi {R_0}^4$ is calculated, and the twist angle θ is found as

$$\theta = \frac{TL}{GJ} = \frac{2TL}{G\pi {R_0}^4} = \frac{2TL}{3G\pi\left({R_0}^2 - \frac{2T}{L\sigma_{\mathrm{Y}}}\right)^2}, \tag{3.9}$$

where G is the modulus of torsional rigidity.

The twist angle θ as a function of time t is presented in Fig. 3.3b for different annealing temperatures τ. The average grain size grows with time in accordance with (3.1), (3.5), (3.6), and (3.8), (3.9) for $K = 4.5 \times 10^6\ \mu\mathrm{m}^2\ \mathrm{s}^{-1}$ (at $T = 300^{\circ}\mathrm{C}$) and $K = 7.6 \times 10^6\ \mu\mathrm{m}^2\ \mathrm{s}^{-1}$ (at $T = 600^{\circ}\mathrm{C}$), $r_0 = 17\ \mu\mathrm{m}$, $k = 3\ \sigma_{\mathrm{Y0}}\ (\mu\mathrm{m})^{1/2}$, $2\tau L/(3\ {R_0}^4 G\pi) = 0.1$, $2\tau/({R_0}^2 L\sigma_{\mathrm{Y0}}) = 1.4$. With increasing grain size, the yield strength decreases in accordance with (3.1). As the maximum shear strength due to the twist deformation reaches the yield strength, a plastic flow zone is formed and the material is softened in accordance with (3.7)–(3.9), until static failure occurs. As expected, a higher temperature leads to the softening, while a lower temperature prevents the transition to the plastic regime.

We conclude that grain growth in metals involves interactions at three different length scales, and thus a multiscale approach is needed for studying the grain growth phenomenon in metals. Using such a multiscale approach, the simple example of the normal grain growth in a simple rod structure at constant temperature was investigated. The same methodology can be applied for more complicated situations such as the prediction of physico-chemical properties during the thermomechanical treatment of structures with complicated geometries.

3.2.2 Multiscale Nature of Degradation and Healing

While the net entropy, as defined by (2.1)–(2.2), grows in most systems in accordance with the second law of thermodynamics, some thermodynamic systems may lead to an increasing orderliness and self-organization, supporting a decrease in entropy. These are thermodynamically open systems that operate far from thermodynamic equilibrium and can exchange energy, matter, and entropy with the environment. Many of these self-organizing systems (such as the Bénard cells in boiling liquid and oscillating chemical reactions) were known a long time ago; however, the universality and generality of the processes involved in these systems was understood only with the works by Prigogine (1961). It is believed that this ability for self-organization of physical systems led to the formation of complex hierarchical chemical and biological systems.

Processes that lead to degradation (wear, corrosion, fatigue, etc) often involve interactions with different characteristic length scales. For example, friction and wear involve interactions of microscale and nanoscale asperities and wear particles, capillary interactions, adhesion, and chemical molecular bonding. In most cases, these interactions lead to irreversible energy dissipation and, therefore, to the production of entropy. However, in certain cases, the entropy production at a particular scale level may be compensated by the entropy consumption at another level.

An interesting example of a self-organizing process is the thermally activated grain growth in metals (Fig. 3.4). It is well known that metal crystals form grains, characterized by different orientations of the lattice (Humphreys and Hatherly 1995). The typical grain size is in the range between microns and millimeters. There is an additional energy associated with the grain boundaries due to the misorientation of the neighboring grains. Therefore, it is energetically profitable for larger grains to grow and to absorb smaller grains, thus reducing the total number of grains and the total boundary area. The ideal state of a perfect crystal with only one grain corresponds to the minimum energy. The grain growth is a thermally activated diffusion-like process with the Arrhenius type of kinetics. For normal isotropic grain growth, theoretical considerations predict a parabolic dependence of the average grain radius r on time

$$r^2 - {r_0}^2 = K_0 \exp\left(-\frac{Q}{RT}\right) t, \tag{3.10}$$

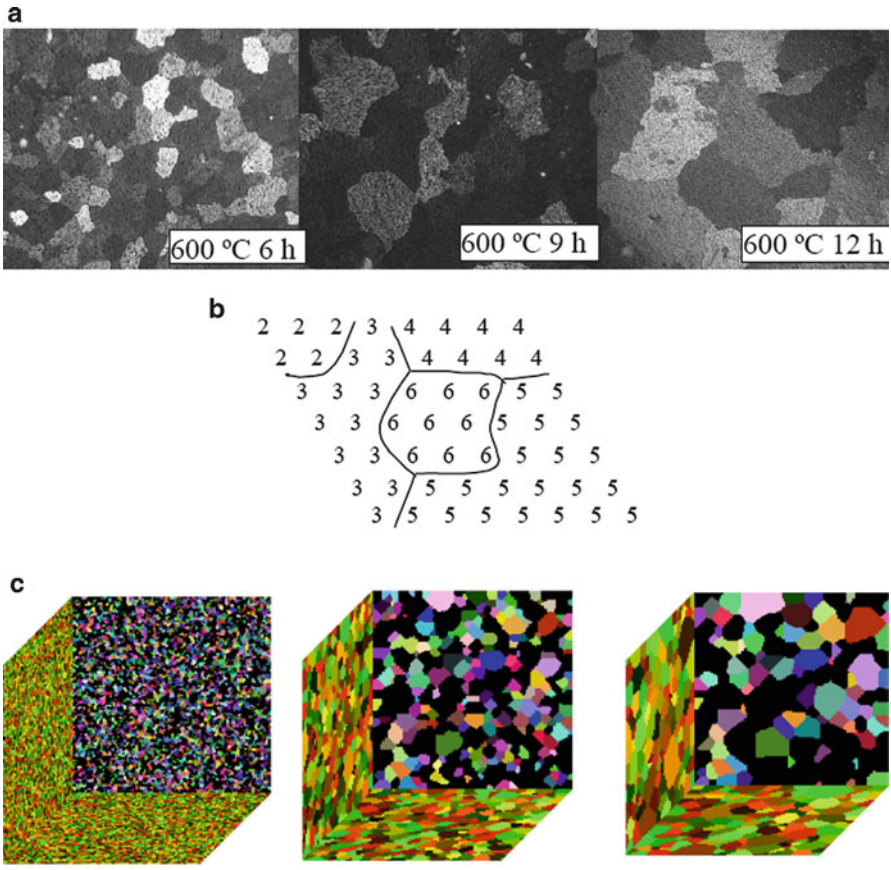

Fig. 3.4 MC simulation of grain growth (**a**) experimental observation of grains in aluminum at different time intervals, (**b**) simulation lattice, (**c**) simulation results for grain growth (Nosonovsky and Esche 2008a)

where Q is the activation enthalpy, R is the universal gas constant, K_0 is a proportionality constant, and r_0 is the initial grain size (Yu et al. 2008).

Modeling the grain growth is a challenging task. Since it is a random process, deterministic modeling is difficult. The Monte Carlo (MC) simulation and Cellular Automata (CA) approaches are often used (Raabe 2000, 2002). CA algorithms describe the spatial and temporal evolution of a complex system by applying deterministic or probabilistic local rules to the cells of a regular lattice. CA algorithms are based on finite difference formulations of local interaction laws. The MC method is based on the use of randomly generated orientation numbers. The lattice is initialized by randomly assigning to each lattice point an integer number representing its orientation. Reorientations are randomly and sequentially attempted for all lattice sites. If a new orientation is characterized by lower energy, then it is accepted (Nosonovsky and Esche 2008a).

A metal with grains represents a typical example of a partially ordered system that occupies an intermediate position between the complete disorder (a random collection of atoms) and complete order (a perfect single crystal). The grain growth is also a self-organizing system, which naturally evolves from a disordered to an ordered state being driven by random thermal fluctuations. Consider an array of N cells, representing lattice cells in the simulation method, with each cell being in one of M microstates. The total number of microstates of this system would then be:

$$\Omega = M^N. \tag{3.11}$$

When the system reaches its final state with all cells having the same orientation, the total number of microstates becomes:

$$\Omega = M. \tag{3.12}$$

Using the statistical mechanics definition of the entropy, one can find the initial entropy S_0 and the final entropy S_f of the system as:

$$S_0 = \ln(MN) = N \ln M = NS_\mathrm{f}, \tag{3.13}$$

$$S_\mathrm{f} = \ln M. \tag{3.14}$$

Based on (3.13) and (3.14), the entropy decreases between the initial and the final states by an amount of

$$\Delta S = (N - 1) \ln M. \tag{3.15}$$

This result constitutes an apparent paradox, because it seems to contradict to the second law of thermodynamics, which states that the entropy of a closed system does not decrease. Another formulation of the paradox is that the *randomness* of thermal fluctuations leads to an increased *orderliness* of the system (Nosonovsky and Esche 2008a).

To solve the paradox, we have to take into account that the system, under consideration, can be studied at different scale levels, and that it is not a closed system. At the macroscale we deal with a continuum system characterized by certain bulk mechanical properties (e.g., yield strength, hardness) dependent on the average grain size. At the macroscale, no change of entropy is expected, $\Delta S_\mathrm{macro} = 0$. At the mesoscale (or microscale) we deal with the grains that tend to grow. Hence, the mesoscale entropy is essentially the configuration entropy and with the increasing grain size it decreases due to the increased orderliness of the system, $\Delta S_\mathrm{meso} < 0$. At the molecular scale (or nanoscale) we deal with the energy barriers for grain growth and random thermal fluctuations. Every time when a lattice site is reoriented, a certain amount of energy is dissipated because the energy barrier must be overcome. However, if the system's temperature is maintained

constant, then the heat is removed from the system due to its contact with the surroundings, and thus the system is not closed. This results in an increase in the system's temperature and entropy, where $\Delta S_{\text{nano}} < 0$. In other words, the random fluctuations at the nanoscale lead to the orderliness increase at the mesoscale, which is compensated by the entropy increase at the nanoscale. The net entropy of the system can therefore be written as

$$\Delta S_{\text{net}} = \Delta S_{\text{macro}} = \Delta S_{\text{meso}} + \Delta S_{\text{nano}}. \tag{3.16}$$

Since $|\Delta S_{\text{nano}}| > |\Delta S_{\text{meso}}|$, the net entropy decreases and the second law of thermodynamics is satisfied (Table 3.2). Note that (3.16) is similar to (2.3) with the only difference that the mesoscale level is included in addition to the macro and micro/nanoscales (Nosonovsky and Esche 2008a).

Therefore, we deal with the two different systems: the physical system, characterized by the thermodynamic entropy, and the simulation system that models the physical system and is characterized by the information entropy. As far as the information entropy of the system, several interesting observations can be made with regard to the self-organizing properties of this system. The numerical CA/MC models consider only the mesoscale structure of the system, and thus only the mesoscale (configurational) entropy change, ΔS_{meso}, can be determined from the CA/MC model. This is the reason of the apparent entropy decrease. The physical system is not insulated; the heat and entropy are removed from the system, so it is not a closed system. However, the numerical CA/MC model does not take into account that aspect, because it is concentrated on the mesoscale description of the physical system. As a result, the second law of thermodynamics is apparently violated in the simulation system in a paradoxical manner. The second law is valid for closed physical systems; however, there is no reason why it cannot be violated for CA/MC models during computer simulation. It should be kept in mind that the work of a computer requires energy dissipation (that is one of the reasons why computer processor is heated and requires permanent cooling), so the decrease in entropy of the information system is compensated by an increase in the thermodynamic entropy.

Our conclusion is that there is a correspondence between the physical system (a metal crystal) and the information system, used for the simulation (for example, CA). However, the physical system is a multiscale system, with the entropy produced at the nanoscale and consumed at the mesoscale, so that the net sum of the entropy grows. The information system simulates only the mesoscale level, leading to the apparent reduction of the entropy. Thus, the second law of thermodynamics is not observed within the computer simulation network. It is noted that such a common dissipative process as the dry friction also has a hierarchical (multiscale) organization (Nosonovsky and Bhushan 2007a; Nosonovsky and Bhushan 2008d, e); therefore, the hierarchical approach to the entropy is important for a broad class of physical systems.

The issue of interest for most applications is the integrity of the macroscale structure (e.g., the absence of cracks) (Table 3.3). The integrity of the macroscale structure can

Table 3.3 Effects of interest at various scale levels for two self-healing mechanisms

	mechanisms			Embedding SMA microwires
		Microcapsule encapsulation		
Self-healing	Physical mechanisms	Interest for application	Physical mechanisms	Interest for application
Macroscale	Solid structure, cracks	Integrity of the solid structure	Solid structure, cracks	Integrity of the solid structure
Microscale	Microcapsules		Microwires	
Nanoscale	Atomic structure		Atomic structure	

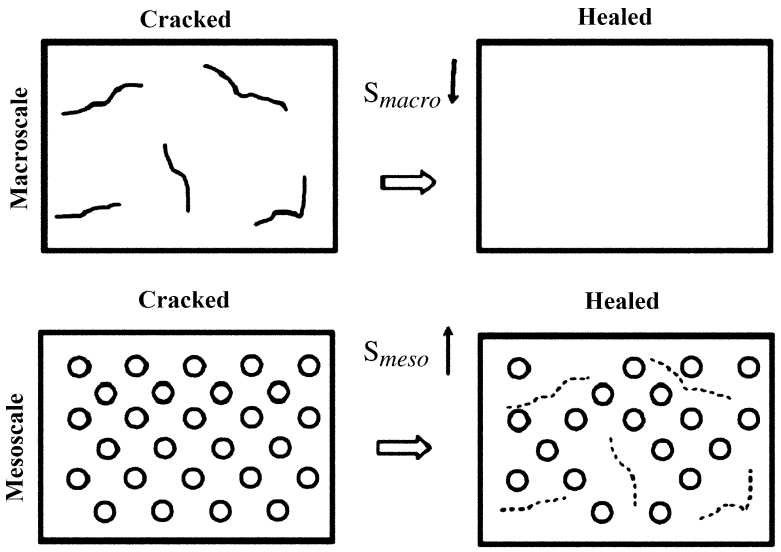

Fig. 3.5 Schematic showing crack healing by embedded capsules at the macro- and microscale levels. Crack healing decreases disorder (and entropy) as observed at the macroscale, while fracture of the microcapsules increases disorder (and entropy) when observed at the mesoscale. Macroscale healing occurs at the expense of the microscale disorder. The effectiveness of the healing mechanism should be studied by relating microstructure parameters to the entropy

be repaired at the expense of the micro- and atomic-scale structures. As an example, let us consider a solid homogeneous body. The nanoscale level corresponds to the vibrations of atoms in the crystalline lattice and is not of interest for us at this point. The mesoscale structures, such as grains, defects, and dislocations correspond to the microscale levels. A perfect single-crystal body with no defects has lower mesoscale entropy, ΔS_{meso}, than a body with such defects. Larger scale defects such as cracks and voids contribute to the macroscale component of the entropy, ΔS_{macro} (Fig. 3.5a).

A material or a surface with a regular microstructure (e.g., a microtextured surface) is more ordered, and thus it has lower mesoscale configurational entropy, ΔS_{meso}, than a material with an irregular microstructure. This can be utilized for

healing of macroscale defects. Suppose there is excess entropy, ΔS_{macro}, associated with the macroscale defects, such as cracks or voids. Healing can be triggered by affecting the mesoscale structure, e.g., by release of the healing agent from microcapsules, which decreases the orderliness of the microstructure and thus increases the entropy for ΔS_{meso}. In the case $\Delta S_{\text{macro}} < \Delta S_{\text{meso}}$, the healing is done by decreasing the macroscale component of entropy on the expense of the mesoscale component (Fig. 3.5b).

3.2.3 Healing Agent Release by Fracture

Encapsulation of a healing agent is used for crack damage repair. When the crack propagates, the capsule ruptures and liquid adhesive is released that can heal the crack. Usually, in the case of polymeric materials, a catalyst should be placed in the structure to initiate solidification of the healing agent. Crack propagation is an irreversible process, because when intermolecular bonds are broken, the energy γ is released irreversibly, so the entropy amount

$$S_{\text{crack}} = \gamma KA/T, \tag{3.17}$$

is produced to create a crack with area A. The coefficient $0 < K < 1$ is the fraction of the dissipated energy Q that is consumed for the creation of the crack, whereas the rest of the energy is dissipated (Nosonovsky et al. 2009).

Another way to introduce the entropy of cracking is to consider the configurational entropy. The ideal state without cracks corresponds to the minimum number of microstates and thus the lowest possible configurational entropy. The crack can be formed in many different ways and the cracked macrostate corresponds to many microstates and excess configurational entropy, ΔS_{macro}. In a similar manner, when a capsule ruptures and its content is released, the configurational entropy grows because mixing occurs. The configurational entropy growth of mixing of two substances is given by:

$$\Delta S_{\text{mixing}} = -R(n_1 \ln X_1 + n_2 \ln X_2) \tag{3.18}$$

where n_1 and n_2 are the amounts in moles of two pure substances, X_1 and X_2 are mole fraction in the solution, and R is the gas constant (Craig 1992). Part of this excess entropy can be consumed for healing the bonds at the crack. The net configurational entropy grows; however, the growth is not due to the cracking but due to microcapsule rupture and an irreversible decrease in the number of filled microcapsules.

If N capsules are ruptured to heal the crack with the area A, the net entropy production is given by the mesoscale entropy of mixing minus the macroscale entropy of crack healing

$$\Delta S_{\text{net}} = \Delta S_{\text{meso}} + \Delta S_{\text{macro}} + N\Delta S_{\text{mixing}} - K\frac{\gamma L}{T} > 0. \tag{3.19}$$

As it has been discussed, the macroscale entropy is reduced on the expense of the mesoscale entropy.

A different technique involves material reinforcement with a shape-memory alloy (SMA), such as NiTi. The shape-memory effect occurs due to the reversible phase transition from the martensite to the austenite phase. Tiny SMA fibers that are embedded into the matrix of the material change their shape (extend) as the crack propagates. Heated SMA fibers restore their original shape and thus close the crack. The macroscale structural integrity of the material is restored at the expense of the increase in the nanoscale entropy due to the phase transition and heat release.

It is noted that we considered a highly simplified model of crack healing. A more sophisticated model should take into account the entropy of the phase transition (in this case, the solidification of the healing agent, $\Delta S_{\text{solidify}}$) and chemical reactions $\Delta S_{\text{chemical}}$ (e.g., with the catalyst), as well as the corresponding chemical potentials. Such a model is presented in the following section.

3.2.4 Healing Agent Release by Heating and Melting

There are two types of self-healing: autonomous and nonautonomous. While autonomous healing is performed without any external intervention, an external stimulation, such as heating, is needed for the nonautonomous healing. The typical example of the nonautonomous self-healing is embedment of a low melting temperature agent that melts after heating, fills cracks and voids, and solidifies after that. The general expression of the entropy is

$$\begin{aligned}\Delta S_{\text{net}} = {} & \Delta S_{\text{heating}} + \Delta S_{\text{melting}} + \Delta S_{\text{chemical}} + \Delta S_{\text{mixing}} + \Delta S_{\text{solidify}} \\ & + \Delta S_{\text{cooling}},\end{aligned} \tag{3.20}$$

where

$$\begin{aligned}\Delta S_{\text{heating}} &= -\int \frac{\mathrm{d}Q}{T}, \\ \Delta S_{\text{cooling}} &= \int \frac{\mathrm{d}Q}{T},\end{aligned} \tag{3.21}$$

are the entropies associated with the heating and cooling process can be given as

$$\begin{aligned}\Delta S_{\text{melting}} &= -\frac{\Delta Q}{T}, \\ \Delta S_{\text{solidify}} &= \frac{\Delta Q}{T},\end{aligned} \tag{3.22}$$

are the entropies of phase transitions and ΔQ is the heat released or consumed during the phase transitions. Since usually the process is not adiabatic and the heat produced during heating and melting is irreversibly dissipated, the net entropy change is

$$\Delta S_{\text{net}} = \int \frac{\mathrm{d}Q}{T} + \frac{\Delta Q}{T_{\text{melting}}} + \Delta S_{\text{chemical}} + \Delta S_{\text{mixing}}. \tag{3.23}$$

To summarize, the self-healing mechanism restores the macroscale structure of a material at the expense of increasing the mesoscale and atomic scale entropy (Nosonovsky et al. 2009).

3.3 Entropy, Degradation, and Healing Rates During Self-Healing

Most models of self-healing use governing equations for crack propagation and for the healing agent that can be used to develop a computational scheme. These systems of equations involve many degrees of freedom (infinite number of degrees of freedom for the continuum models and very high finite number of degrees of freedom for the computational models). In this section, we suggest a different approach and develop a system of equations for degradation parameters with a low number of degrees of freedom.

3.3.1 Entropy and Degradation

Consider a process characterized by a degradation parameter ξ, for example, the wear volume or the total area of the cracks. The rate of degradation in many cases is proportional to the rate of entropy

$$\dot{\xi} = B\dot{S}, \tag{3.24}$$

where B is the degradation coefficient (Bryant et al. 2008).

Taking the degradation parameter equal to the wear volume, $\xi = w$, (3.24) yields the Archard wear law

$$\dot{w} = k\frac{WV}{H}, \tag{3.25}$$

where $k = \mu HB/T$ is the wear coefficient, and H is the hardness (Nosonovsky and Bhushan 2009). For crack propagation, (3.24) is equivalent to (3.17) if $B = T/(\gamma K)$.

Thus, the physical meaning of (3.24) is that a constant fraction of the dissipated energy at a given temperature is consumed for the degradation, and therefore the rate of degradation is proportional to the rate of entropy.

3.3.2 Degradation and Healing

Healing is characterized by a healing parameter, ζ, for example, the volume of released healing agent. The rate of healing or decrease of degradation, $\dot{\xi}_{\mathrm{h}}$, is proportional to the amount of healing material, and to a function of ξ. The rate of release of the healing agent, $\dot{\zeta}$, is a function of the rate of increase in the degradation, $g(\dot{\xi}_{\mathrm{d}})$, and the rate of consumption of the healing agent. For example, the number of fractured microcapsules is proportional to the length of newly created cracks, and thus the amount of the healing agent depends on the length of the newly created cracks minus the amount of consumed healing agent

$$\dot{\zeta} = g(\dot{\xi}_{\mathrm{d}}) - C\dot{\xi}_{\mathrm{h}}, \tag{3.26}$$

where C is a constant. Thus, the rate of crack healing depends on the amount of the healing material and available crack length. Therefore, we have the system of equations

$$\begin{aligned} \dot{\xi} &= \dot{\xi}_{\mathrm{d}} - \dot{\xi}_{\mathrm{h}}, \\ \dot{\xi}_{\mathrm{h}} &= f(\xi)\zeta, \\ \dot{\zeta} &= g(\dot{\xi}_{\mathrm{d}}) - C\dot{\xi}_{\mathrm{h}}. \end{aligned} \tag{3.27}$$

The entropy is related to the degradation rate according to (3.24). Since the degradation rate involves two components, the net entropy also involves two terms: the term responsible for the degradation and the term responsible for the healing.

$$\Delta S = \Delta S_{\mathrm{d}} - \Delta S_{\mathrm{h}}. \tag{3.28}$$

The origin of these two terms is different. While the degradation term is given by (3.24), the healing term is related to the process of repair of the damage, for example, due to an encapsulated healing agent.

According to some studies, there are five steps in the self-healing cycle: (1) the material is subjected to gradual deterioration, for example, by dynamic loading that induces microcracks; (2) the hollow microcapsule or the fiber contains self-repair fluid; (3) the fibers require a stimulus to release the repairing chemical; (4) a coating or fiber wall must be removed in response to the stimulus; and (5) the fluid must promote healing of the composite damage (Wool 2008). For a truly autonomous self-healing material, the third step may be omitted, as the damage itself serves as the stimulus (Fig. 3.6a). The scheme suggested by (3.26) scheme is intended to

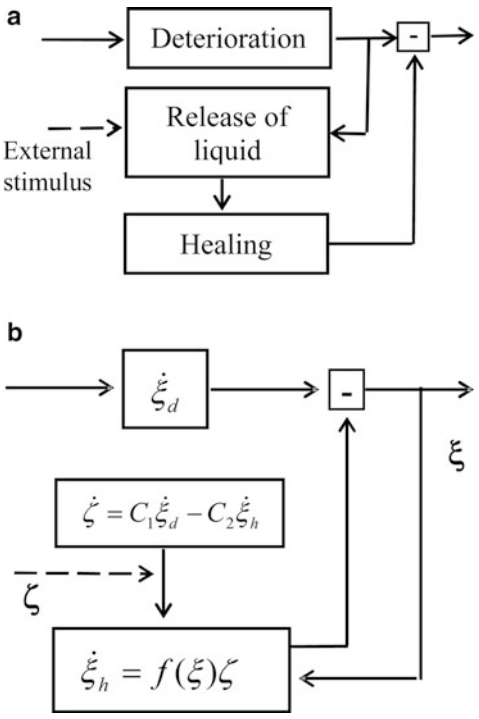

Fig. 3.6 Schematic of (**a**) the self-healing process and (**b**) its representation with (3.26)

capture this process (Fig. 3.6b). It is noted that unlike the approach that uses continuum constitutive equations with infinite degrees of freedom (Wang et al. 2007a, b, c), our method reduces the problem to only two degrees of freedom.

The criterion for self-healing is that the rate of healing is higher than the rate of degradation

$$\dot{\xi}_{\mathrm{h}} \geq \dot{\xi}_{\mathrm{d}}. \tag{3.29}$$

The function $f(\xi)$ involves the dependence of the healing rate on the total length of the cracks or other damage, because the same amount of the healing agent can result in a different rate of repairing the crack. Assuming simple constant dependencies $f(\xi) = B$, $g(\dot{\xi}_{\mathrm{d}}) = D$, and a constant degradation rate (e.g., a steady growing crack), $\dot{\xi}_{\mathrm{d}} = A$, the system of (3.27) yields

$$\begin{aligned} \dot{\xi}_{\mathrm{h}} &= a\mathrm{e}^{-BQ} + \frac{AD}{C}, \\ \dot{\xi}_{\mathrm{h}} &= B\zeta, \\ \dot{\xi} &= A\left(1 - \frac{D}{C}\right) - a\mathrm{e}^{-BQ}, \end{aligned} \tag{3.30}$$

where a is a constant of integration, and in the steady state limit ($a = 0$), the condition (3.29) yields $D/C > 1$. In other words, the crack is healed if more healing agent is released per unit length growth of the crack (constant D) than consumed per unit length of the healed crack (constant C) (Nosonovsky et al. 2009).

3.4 Validation of the Model for Self-Healing Al Alloy

Lucci et al. (a, b, c) investigated both numerically and experimentally self-healing of aluminum alloy 206 matrix reinforced with carbon fiber microtubes filled with Sn60Pb40 solder. The melting point of the solder is between 189 and 190°C. The inside and outside diameters of the tubes were 2,185 μm and 3,950 μm, respectively, their length was 75 mm, the spacing between the tubes was 3 mm on average, and a total of seven sealed tubes were placed. A hole was drilled in the specimen. This sample was then heated above 300°C for 5 min and quenched to ambient temperature. After a series of experiments, the crack was filled with the solder either completely or partially. These experiments indicated the importance of the factors that control filling of the crack by the liquid agent. These factors include the amount of available solder and the wettability of the holes with liquid solder, and the proximity of holes to healing agent as well as the diameter of holes (Fig. 3.7).

The volume of released liquid solder depends on the number of fractures microtubes and the volume of solder in every microtube. A fraction of this volume is available for healing and the healing process depends also on the size of the crack. The degradation parameter ξ in this case is the volume of the crack, while the healing parameter ζ is the volume of available liquid solder. The differential equations for the crack volume and the volume of available healing agent are given by

$$\begin{aligned} \dot{\xi} &= -f(\xi)\zeta, \\ \zeta &= g_0 + C\xi. \end{aligned} \tag{3.31}$$

The first equation states that the volume of the crack decreases with the rate proportional to the volume of available healing agent, with g_0 is the maximum volume of the healing agent. The second equation states that the volume of available healing agent decreases as the agent is consumed for healing. The system of (3.31) can be naturally derived from (3.18) with a number of natural assumptions. These assumptions include zero degradation rate, $\dot{\xi} = -\dot{\xi}_h$ (the crack does not expand after it was initially created) and $g = 0$.

In the case when all available solder is consumed, a constant dependency $f(\xi) = B$ is assumed and the system of (3.31) reduces to one simple equation

$$\dot{\xi} = -B(g_0 + C\xi), \tag{3.32}$$

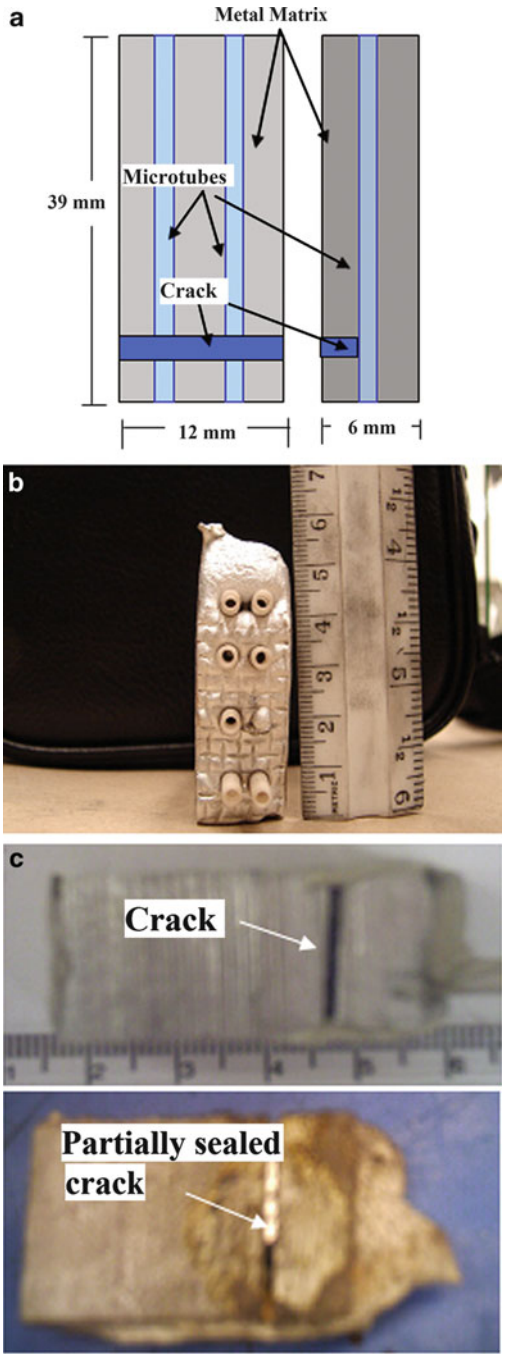

Fig. 3.7 Self-healing Al composite with microtube reinforcement (**a**) geometry of the sample, (**b**) front view, (**c**) before and after the healing (Lucci et al. 2008a, b, c)

which can be immediately solved as

$$\xi = -\frac{g_0}{C} + D\exp(-BCt). \tag{3.33}$$

The fist term is the steady-state solution corresponding to the degree of degradation after the healing is completed. The second term is the transient part of the solution. It is beneficial for the system to have a high ratio of g_0/C (maximum volume of the healing agent, g_0, over the rate of its consumption, C). We can conclude that the model is consistent with the experimental data.

3.5 Summary

Conventional engineering surfaces tend to degrade and become worn due to increasing thermodynamic entropy, which is a consequence of the dissipation during sliding contact. Most biological tissues, however, have the ability of self-healing. In order to embed the self-healing property into engineered materials, special efforts should be made. From the thermodynamic point of view, self-healing is a result of decreasing entropy. This is possible in the case of a special organization of these systems. One possibility is in the case when the system has a special multiscale structure with the dissipation occurring at one level of the system and self-organization occurring at a different hierarchy level. This can be achieved, for example, by embedding microcapsules or microtubes with a healing liquid to prevent crack propagation. We also suggested a simple system of equations that describes the degradation and healing process and provides a criterion for self-healing.